

# Deformation Monitoring of a Steel Structure Using 3D Terrestrial Laser Scanner (TLS)

Jatmiko<sup>1</sup>, Panos Psimoulis<sup>2</sup>

<sup>1</sup> Ministry of Agrarian Affairs and Spatial Planning, Republic of Indonesia

<sup>2</sup> Nottingham Geospatial Institute, The University of Nottingham, United Kingdom  
[jatmiko@bpn.go.id](mailto:jatmiko@bpn.go.id), [panagiotis.psimoulis@nottingham.ac.uk](mailto:panagiotis.psimoulis@nottingham.ac.uk)

**Abstract.** Terrestrial Laser Scanner (TLS) offers a new approach of deformation analysis. Different from conventional equipment such as Global Navigation Satellite System (GNSS) and Total Station (TS), the entire surface of observed structure can be analysed by contactless measurement. However, until recently the application of laser-scanner is still limited to long-term deformation monitoring. Using TLS to monitor dynamic response faces some challenges, such as scan time delay and its data characteristic. This project proposed helical mode to solve these issues and tested the proposed solution in a high-rise artwork deformation monitoring case, the Aspire Sculpture in Nottingham. The result showed that scan time delay can be solved. Then TLS can be used to observe the sculpture dynamic deformation. New approach of point cloud processing was introduced in order to extract the deformation. Using this approach, laser-scanner can be used to monitor dynamic motion of a structure.

## 1. Introduction

Terrestrial Laser Scanner (TLS) has been introduced in deformation monitoring the last 15 years. Lichti et al. (2002) did the earliest attempt using TLS for structure deformation monitoring. They used TLS to monitor bridge deformation on loading test and compare the result with the result achieved using photogrammetry technique. Schneider (2006) used TLS to determine bending line of television tower and to observe the deformation of dam water. For long-term deformation monitoring, laser scanner has been proven to be a reliable technique. On the other hand, monitoring dynamic motion, such as structural response, is still a very challenging task. Even though, there are TLS with the capacity to scan in high sampling-rate ( $>1\text{Hz}$ ), there are restrictions in the function of the TLS, which limit their application for monitoring of dynamic motion. Such a difficulty is the scan time delay between the successive scans, causing complication in the time-stamping of the scans and generally in monitoring moving or oscillating object.

## 2. Literature Review

In deformation monitoring project, there are two steps that are usually followed by researchers or surveyors. These steps are measurement at field and displacement extraction itself. In deformation work, monitoring is typically observing several defined points prior to the observation and then comparing these points at different epochs. Using TLS allows getting massive points as point clouds. This becomes a challenge in the process since it may be difficult to assess some fix benchmarks on the surface of the deforming area (Tsakiri et al., 2006).

Deformation monitoring using TLS is comparing same surface at different epochs. The accuracy of surface reconstruction based on point cloud data determines deformation-monitoring accuracy. Furthermore, sometimes the surface should be reconstructed from some scenes. One of the familiar methods of surface reconstruction from various scenes in

deformation monitoring is Iterative Closet Point (ICP). A brief explanation of ICP approach in deformation monitoring can be found in Teza et al. (2007), they used ICP algorithm to do automatic calculation of landslide displacement field. This method also can be found in Schneider (2006); Sarti et al. (2009); Pesci et al. (2011); Pesci et al. (2012); and Teza and Pesci (2013).

Deformation extraction can be achieved using different approach. In Monserrat and Crosetto (2007), the authors identified some methods commonly used to extract deformation from point cloud data. The deformation values can be obtained by directly comparing Digital Elevation Model (DEM) at different epoch measurements. In Schafer et al. (2004), the authors used Delaunay-Triangulation to create regular surface from point cloud data of a platform of hydropower station at different epoch measurements to achieve its deformation. In Teza et al. (2007), the authors proposed a procedure to calculate landslide displacements called the Piecewise Alignment Method (PAM). Base on this procedure, the first data of the point clouds processed become a first complete landslide model. Polynomial modelling was used as an approach to transform point cloud to surface model. This complete landslide model will be used as reference to calculate the deformation. Other deformation extraction that used Digital Terrain Model (DTM) approach can also be found in Wilkinson et al. (2012).

The approach that is commonly used in deformation monitoring extraction takes advantage of the observed object's shape. Regular objects, such as circle, ellipse and cylinder have mathematical models. These mathematical models are used to reconstruct the object from point clouds. Then the deformation is extracted from created model by comparing one model to others. In terms of achieving good quality of deformation result, choosing the right mathematical model is fundamental. How circle-fitting model was used to detect deformation can be seen in Schneider (2006), and Teza and Pesci (2013). While in Wei et al. (2014), the authors used ellipse-fitting model as model basis which is similar to that of Schneider (2006). In Vezočník et al. (2009), the authors used cylinder model to detect displacement of observation pillars of underground gas pipeline. Sarti et al. (2009) observed a structure that more complex, a parabolic. In Liu et al. (2014), the authors performed deformation monitoring on a more complex structure, railway track.

Previous studies have been made, focusing on application of TLS on dynamic deformation monitoring. For instance, Hong and Laefer (2014) used TLS to capture the dynamic displacement of a structure, where they tried to limit the problem of the time stamping by restricting the monitored area, which reduced the time delays of the successive scans but not solved the problem, as there were time delays and gaps on the captured data of. In this study, we used a 3D TLS functioning in helical mode and modified version of the TLS interface, allowing for automatic time-stamping of the scans, to monitor the dynamic response of a steel structure. The results have shown that the 3D TLS can detect the motion of the structure by using the appropriate filtering techniques.

### **3. Methodology - Measurements**

#### **3.1 Faro Laser Scanner Focus<sup>3D</sup> 120**

For this study, we used FARO Focus<sup>3D</sup> laser scanner, which has helical mode function, where the laser scanner is forced to scan the profile of the object without any horizontal rotation. Furthermore, thanks to the open interface of the laser scanner, we developed an option to extract the time-stamping of its scan with 1 $\mu$ s resolution. Finally, from the scan of the helical mode, we were able to extract the coordinates of every point in a local coordinate system, where the TLS is the origin, and the time-stamping of the measurement. Figure 1 shows Faro

Focus<sup>3D</sup> attached to Helical Adapter with Automation Test Box (left) and Faro open interface application (right). The application will be used to export helical mode data into positions and their time-stamping in an ASCII file.

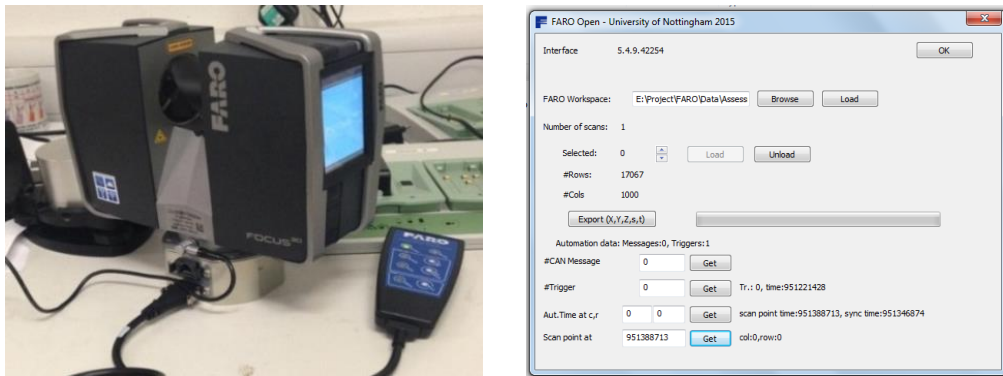


Figure 1: (left) Faro Focus<sup>3D</sup> and (right) Faro open interface application

### 3.2 Measurements and Deformation Extraction



Figure 2: (left) Wall of National Geospatial Building (NGB) and (right) Aspire Sculpture

An external 11m tall wall of Nottingham Geospatial was scanned several times with different distances as experimental test (Figure 2 left), from distances ranging from 6 to 60m. By measuring the wall from different distances, correlation between laser scanner distance to observed object and its accuracy can be assessed. Analysing the accuracy of points at different level along the wall will confirm whether angle between observed point and laser scanner's horizontal line is affecting the measurements accuracy or not. This experimental would not only reveal the correlation between distance, angles and its accuracy, but also the appropriate way to extract the displacement from helical data for dynamic deformation monitoring purposes.

Aspire Sculpture (figure 2 right) in Nottingham has 60m high, consist of 8m of concrete foundation and 52m steel structure. It presumed to be designed as vertical as possible. However due to its construction process and accumulation of environmental conditions like climate, Sun radiation and seismic activity, the bending line of the tower could be changed. This long-term deformation monitoring method took advantage of the shape of the sculpture. In general, the sculpture shape is cylinder. This bending line determination case is similar with what had been done by Schneider (2006). A Python program was written to extract the long-term displacement, bending line determination. The circle-fit algorithm only used x and y data (2D layer) and ignoring the z value. The circle fitting was solved using optimise least square approach.

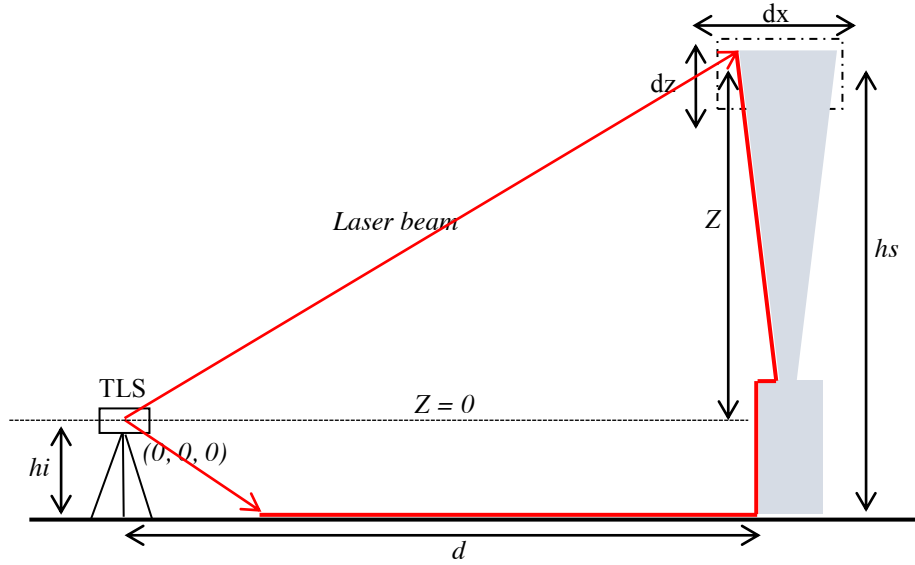


Figure 3: TLS and scanned structure

In order to design a program to extract dynamic deformation, the first thing to do was studying how helical mode records its data. Figure 3 shows the correlation between helical mode scanning area, its coordinate system and the structure. Where  $h_s$  is height of the structure/observed point,  $h_i$  is height of instrument (TLS),  $d$  is distance between TLS and the structure,  $Z$  is height of the structure in TLS coordinate system,  $(0, 0, 0)$  is origin of coordinates system of TLS. The  $dx$  and  $dz$  are distances to define the area of the structure that is to be analysed or its displacements determined. Correlation between laser scanner position and the structure during measurement was important to be considered in order to define a filtering procedure in the program. Filtering was needed since the laser scanner data does not only consist of the observed structure but also other objects and noises. There two steps in the filtering process. The First step is to remove the first-twenty of profiles to ensure there are no noise profiles as FARO Focus<sup>3D</sup> laser scanner we used recorded noises at first-twenty vertical rotations. The second step is to remove half of total profile. When measuring using helical mode, laser scanner scans two profiles in single vertical rotation. One profile belongs to be the observed structure, while another belongs to be any object in backside of laser scanner.

Displacement was calculated using several points that represent a point of observed structure ( $\sim 0.2m$  zone). This approach gives better precision than using single point of helical mode data. This could be explained as obtaining a single point by averaging several points representing that single point, thus, minimising the error every single point has. Average of those points was calculated for each profile. Then the displacements were calculated from these averaged points using the first point as a reference. For  $\sim 0.2m$  sliced profile, each

profile within this area should have same number of points but sometimes some profiles have less number of points than they should have. This could be effect of ranging noise of the laser scanner. When the percentage of reflection of laser beam is small due reflectiveness of the scanned surface, laser scanner ignores this point. The average point should be calculated using same number of points for each profile to prevent this noise propagates to accuracy of the displacements significantly. Profiles with number of points different with other (its majority number) should be removed before calculating the average. A filtering based on *mode* statistic data was applied in the Python program to filter these unwanted profiles. Another thing that should be looked carefully before calculating the average is to make sure that each row in the sliced profile has the same number of profiles.

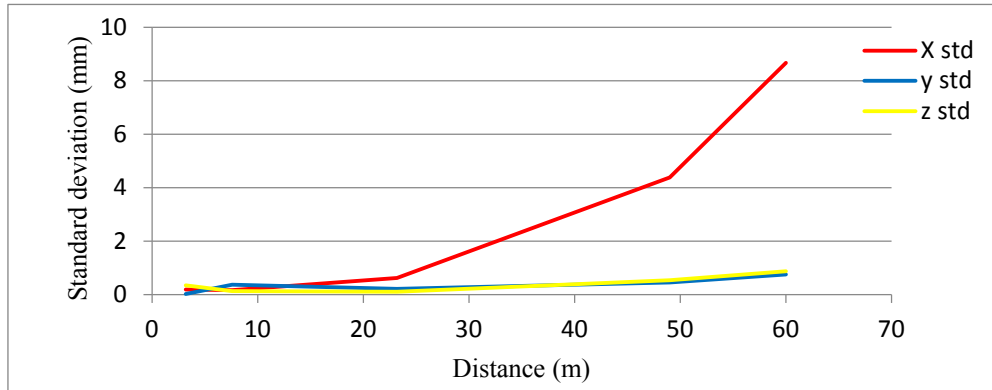


Figure 4: Estimate standard deviation and distance

Accuracy of helical mode was accessed using wall experimental data. By assuming that the wall was stable and there was no local seismic activity during measurements that affected the wall, displacement of wall should equal to zero. The wall was scanned several times from different distances, 3.2, 7.5, 23.2, 49 and 60m. The estimate standard deviation of displacements from these measurements can be seen in Figure 4. Standard deviations were calculated from displacement of point of 5m level observed from varying distances. Distance affected standard deviation significantly in x direction with value range between 0.1 to 8.6mm. In y- and z-directions, distance between target and station did not significantly affect the standard deviation (range between 0.1 to 0.8mm) since the y and z values in different distance stations did not change. This variation of standard deviation was due to ranging error and noise of the laser scanner propagated with varying x, y and z values. The correlation between distance and accuracy can be seen clearly in x-direction and this could be used to estimate laser scanner accuracy. For deformation monitoring expecting accuracy approximately 2mm, the distance between station and scanned object being observed should be approximately 25m. In range of 60m, the expected displacement should be more than 10mm.

## 4. Results and Discussion

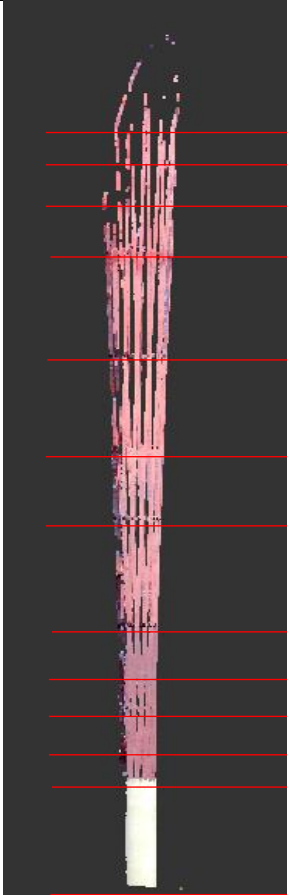
### 4.1 Aspire Sculpture Long-term Deformation

Table 1 shows Circle fitting result of Aspire Sculpture. All circle of steel part was sliced near circular or ring section of Aspire that connect one column with others, except for height of 50 and 53 m. The top of sculpture cannot be modelled due to the shape of sculpture at the top is not a full cylinder. The quality of distribution of point cloud used for each circle can be seen in standard deviation of radial distance. For sculpture part made from concrete, standard

deviation was 1 millimetres, while for sculpture part made from steel was between 15 to 32mm. A big different of quality of point cloud between them can be explained by the concrete part has uniform shape and smooth surface, while steel part has many columns with different sizes of mast.

Between the concrete and steel material there was approximately 40mm of displacement in both directions. This value cannot be confirmed. It was due to deformation during construction that steel structure was not centred prissily to concrete pillar or it is due to deformation caused by aging effect. The other heights show variation of deviations in both directions. Between 10 and 30m level, the deviation in both direction relatively small, but in height above 30m to the top of sculpture the deviation was bigger. This can be explained by the design of sculpture with bigger shape and thinner mast at the top. It makes them more vulnerable. By assuming there was no temporal forces that affected the sculpture during measurement such wind, sun radiation or local seismic activity, and assuming that the sculpture was constructed truly vertical, it can be concluded that the sculpture vertical axis has changed compare to its initial design. There was a deviation between mass centre of structure at the foundation and at 53m level approximately 42mm and 13.8mm in x- and y-directions respectively. This deviation was approximately  $0.14^\circ$  of displacement to its vertical axis.

Table 1: Circle fitting result of Aspire Sculpture

Cut of point cloud into thin layers/circles at different heights	Height of points (m)	Centre of circle		Radian (m)	Standard deviation (mm)	Material
		$X_m$ (m)	$Y_m$ (m)			
	53	11.761	11.055	2.414	16	Steel
	50	11.710	11.054	2.246	15	Steel
	45	11.693	11.083	1.997	32	Steel
	37.7	11.681	11.121	1.726	26	Steel
	31.22	11.699	11.144	1.495	30	Steel
	26.26	11.702	11.154	1.342	30	Steel
	22.25	11.698	11.148	1.223	28	Steel
	18.8	11.692	11.149	1.141	30	Steel
	15.7	11.687	11.141	1.079	25	Steel
	13	11.687	11.145	1.041	28	Steel
	10.5	11.681	11.140	1.013	24	Steel
	8	11.717	11.187	1.098	1	Concrete
	0	11.719	11.193	1.102	1	Concrete

## 4.2 Aspire Sculpture Dynamic Motion

Several attempts of helical mode measurement were done due to the sculpture's shape characteristic which makes all part of it at every level difficult to be scanned using this profiler mode. First attempt was done with distance between laser scanner and sculpture was 40m, in 22<sup>nd</sup> June 2015. Local weather forecast showed wind speed was 19 km/h. This measurement used  $\frac{1}{4}$  and 3x of resolution and quality respectively. This gave a 24 profiles per second or 24Hz sampling rate data. Not all part of structure from the bottom to the top could be scanned. The second attempt was done in 24<sup>th</sup> June 2015 while the wind blew with a speed of 14 km/h. Second measurement was done using approximately 18m of distance. The measurements used resolution and quality setting of  $\frac{1}{2}$  and 3x respectively. It gave 12Hz of sampling rate. This laser scanner setting had better resolution than the first attempt setting. It made the number of points of the second attempt more than the first attempt. Figure 5 shows raw data plot in 3D and its xz-projection of second attempt.

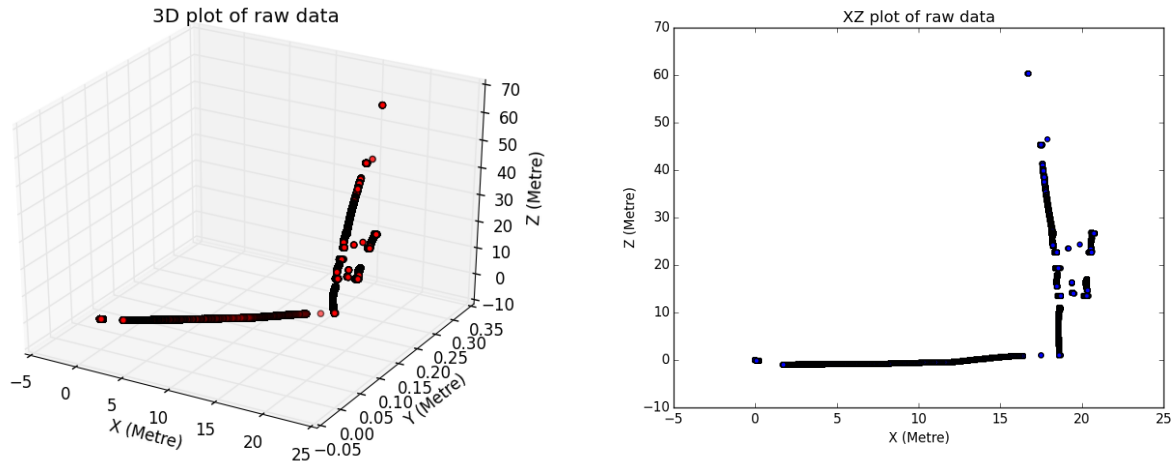


Figure 4: A typical data-set of the point-cloud of the its profile scanned with FARO Focus3D laser scanner (second attempt)

Table 2: Second attempt result (24<sup>th</sup> June 2015)

Height (m)	Recorded profile	Profile used	Profile unused	Total points	Estimate standard deviation			Decision
					$\sigma_x$ (mm)	$\sigma_y$ (mm)	$\sigma_z$ (mm)	
5*	100%	58.06%	41.94%	33	0.5	0.3	0.1	No
10	100%	39.27%	60.73%	20	0.7	0.3	0.4	Oscillated
15	-	-	-	-	-	-	-	-
20	-	-	-	-	-	-	-	-
25	100%	79.19%	20.81%	12	1.5	0.3	1.9	Oscillated
30	99.83%	48.79%	51.04%	10	1.8	0.3	2.9	Oscillated
35	89.19%	19.76%	69.43%	8	2.2	0.3	4.4	Oscillated
40	58.27%	19.76%	38.51%	6	2.6	0.3	5.8	Oscillated
45**	97.90%	41.53%	56.38%	7	1.3	0.3	3.3	Oscillated
50	-	-	-	-	-	-	-	-
55	-	-	-	-	-	-	-	-
60***	17.06	6.25%	10.81%	2	14.3	0.3	10.4	Oscillated

\*concrete part \*\*ring of sculpture

\*\*\*top part of sculpture



Table 2 summarises the displacement of sculpture for every 5m level. The percentage in recorded profile, profile used and profile unused columns were calculated from the total data of structure recorded from the measurement (the number of line inputted to the laser scanner setting). Total points column data could be used for calculating the average point. In general, the displacement magnitude increased as level increased, except for height of 45m as at this level the scanned sculpture was not the mast likes at other levels, but ring of the sculpture that connecting all columns. The number of profiles could be processed decreased due to sculpture shape characteristic and laser scanner ranging limitation. As the time-series still have ranging error and ranging noise, in order to decides whether the trend in time-series was systematic error or the structure displacement, an analysis should be carry out. This analysis was done by comparing estimated standard deviation of the structure with estimated standard deviation of laser-scanner due to distance (Figure 4). For distance between laser-scanner and structure approximately 18m, the estimate standard deviation for x-direction to be categorized as oscillated should be more than 0.5mm. While for z value the comparison should use its height instead of distance. For example, for point of 10m height, the judgement should use estimate precision of 10m distance instead of 18m, should be bigger than 0.3mm. The highlighted standard deviations mean that at these levels the structure was oscillating.

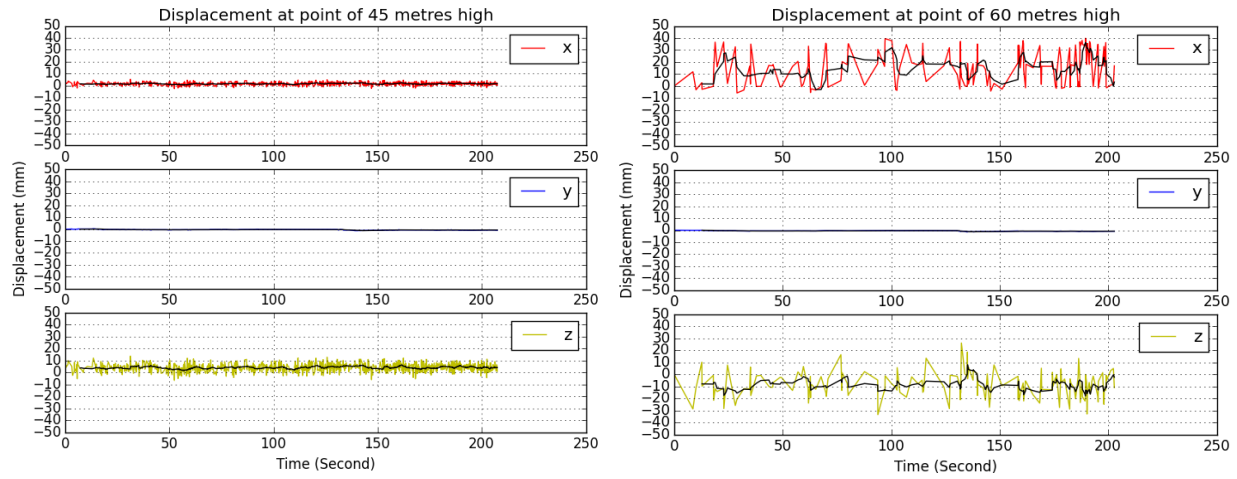


Figure 6: Time-series of displacements and its moving average of second attempt (45 and 60m level)

Figure 6 shows time-series of displacements at 45 and 60m level and their 20-window moving average. At 60m level, the time-series has many gaps. This could be explained by structure characteristic and laser scanner limitation made not all of the structure profiles could be recorded and processed for deformation analysis. At higher points, the displacement was expected to be bigger than one occurred at lower points, but at 45 m height showed the opposite. The explanation is that the effect of wind to sculpture displacement could be bigger at the masts, but it then drops at the rings that connecting all different part of sculpture into a full sculpture shape. From the time-series, amplitude in z-direction was bigger than in x-direction but this is not due to displacement of the structure. The displacement at this point in x-direction was small. While in z-direction, the displacement was also small but the laser-scanner error and noise were propagated maximum at this point and made the magnitude of time-series in z-direction bigger than in x-direction. The largest displacement of the sculpture was at the top part (60m). In x-direction, the amplitude of the displacement was approximately 40mm. Semi-static was detected clearly at approximately 140 seconds until the end of time-series.

Using time-series of displacement the frequencies of dynamic deformation could be driven (Psimoulis and Stiros, 2008). Using Discrete Fourier transform (DFT), the second attempt



data was processed in order to reveal estimated sculpture displacement frequencies. The second attempt data was chosen since it has most complete data from bottom to the top of structure. The spectral analysis was only focused on displacement in x- and z-directions as the dynamic movement of structure in y-direction was not recorded by helical mode. The second attempt was using resolution and quality setting of  $\frac{1}{2}$  and 3x. It gave 12Hz of sampling rate data. Therefore, the maximum frequency that can be detected by this spectral analysis is 6Hz. The spectral analysis focused on highest peak in the spectrum corresponding with the structure dynamic motion. At point of 45m level, the peak of frequency detected was 4Hz. While at the point of 60m level the peak was 0.25Hz (Figure 7).

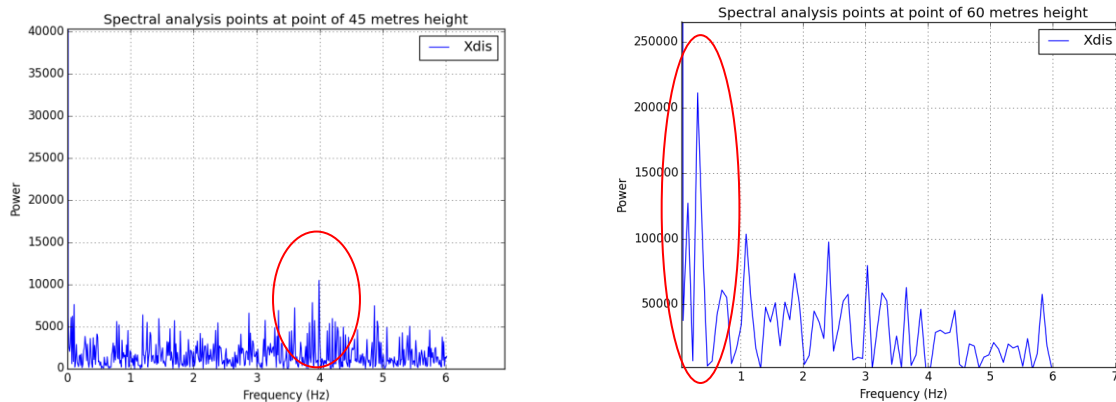


Figure 7: Spectral analysis of point 45 and 60m level

To sum up, frequency approximately 0.25 Hz was detected at points 10, 25, 40 and 60m level. Frequency of 1.7 Hz and 4 Hz were detected at point of 30 and 45m level. This variation of frequency could be due to the structure shape. The mast responded to the wind power differently with varying level. However, most levels detected a frequency of 0.3Hz. For the point of 45m level, the frequency was the biggest. It could be due to that the laser scanner observed the ring instead of the columns or the mast like other levels. The vibration in all masts was accumulated in the ring uniting the masts. It could be concluded that the ring made the magnitude of the displacement decrease while it accumulated the frequency of vibration.

## 5. Conclusion

Scan time delay of laser scanner could be solved by turn off the horizontal rotation using FARO's helical mode. FARO provides open source libraries, FARO LS SDK and FARO Open Interface, which allow user to create tool to handle laser-scanner and access all information in FARO data. Helical mode accuracy had been tested using simple procedure. In short-range measurements with distance less than 25m, it can achieve up to millimetres precision.

A full monitoring of Aspire sculpture deformation had been demonstrated in this project. This monitoring observed long-term, semi-static and dynamic deformation of the longest standing artwork in United Kingdom. The first monitoring was to inspect the long-term condition of the sculpture. Using standard operation of laser scanner, the bending line of the sculpture had been determined. The bending line of this structure moves approximately  $0.14^\circ$  to direction where sculpture has the highest side (Southeast). The dynamic displacement recorded approximately 40mm at the top of structure during measurement when wind blew with speed of approximately 14 km/h. The observation also detected the highest frequency of 4Hz.

FARO Open developed in this project was designed to extract position and time only. Yet in laser scanner, there are two major errors, ranging error and ranging noise. By exporting the reflectiveness value, the ranging noise may be able to be modelled to increase the quality measurement. This project used C++ in order to develop FARO Open application and Python for deformation extraction. It would be better to develop single application for both tasks. The method presented in this project needs to be verified using other sensors.

## References

- Hong, L, T, & Laefer, D, F 2014, 'Using terrestrial laser scanning for dynamic bridge deflection measurement', *Istanbul Bridge Conference*, Istanbul, 2014, viewed 21 July 2015, <http://istanbulbridgeconference.org/2014/ISBN978-605-64131-6-2/papers/060.pdf>
- Lichti, D, D, Gordon, S, J, Stewart, M, P, Franke, J & Tsakiri, M (2002), 'Comparasion of digital photogrammetry and laser scanning', Viewed 7 November 2014, [http://www.researchgate.net/publication/245716767\\_Comparison\\_of\\_Digital\\_Photogrammetry\\_and\\_La\\_ser\\_Scanning?enrichId=rgreq-b68fd2ba-1d6d-4f0f-b05f-bf9166f11a01&enrichSource=Y292ZXJQYWdlOzI0NTcxNjc2NztBUoxNDI5NjQyMTQ5OTY5OTNAMTQxMTA5NjczMzc4Nw%3D%3D&el=1\\_x\\_2](http://www.researchgate.net/publication/245716767_Comparison_of_Digital_Photogrammetry_and_La_ser_Scanning?enrichId=rgreq-b68fd2ba-1d6d-4f0f-b05f-bf9166f11a01&enrichSource=Y292ZXJQYWdlOzI0NTcxNjc2NztBUoxNDI5NjQyMTQ5OTY5OTNAMTQxMTA5NjczMzc4Nw%3D%3D&el=1_x_2)
- Liu, C, Li, N, Wu, H, & Meng, X 2014, 'Detection of high-speed railway subsidence and geometry irregularity using terrestrial laser scanning', *American Society of Civil Engineers*.
- Monserat, O, & Crosetto, M 2007, 'Deformation measurement using terrestrial laser scanning data and least squares 3D surface matching', *ISPRS Journal of Photogrammetry & Remote Sensing*, pp. 142–154.
- Pesci, A, Bonali, E, Galli, C & Boschi, E 2012, 'Laser scanning and digital imaging for the investigation of an ancient building: Palazzo d'Accursio study case (Bologna, Italy)', *Journal of Cultural Heritage*, pp. 215–22.
- Pesci, A, Casula, G & Boschi, E 2011, 'Laser scanning the Garisenda and Asinelli towers in Bologna (Italy): detailed deformation patterns of two ancient leaning buildings' *Journal of Cultural Heritage*, pp. 117–127.
- Psimoulis, P, A, & Stiros, S, C 2008, 'Experimental assessment of the accuracy of GPS and RTS for the determination of the parameters of oscillation of major structures.' *Computer-Aided Civil and Infrastructure Engineering*, pp. 389–403.
- Sarti, P, Vittuari, L & Abbondanza, C 2009, 'Laser scanner and terrestrial surveying applied to gravitational deformation monitoring of large VLBI telescopes primary reflector', *Journal Of Surveying Engineering*, pp. 136-148.
- Schafer, T, Weber, T, Kyrinovič, P, & Zámečniková, M 2004, 'Deformation measurement using terrestrial laser scanning at the hydropower station of gabčíkovo', *FIG Regional Central and Eastern European Conference on Engineering Surveying*. Bratislava, 2004.
- Schneider, D 2006, 'Terrestrial laser scanning for area based deformation analysis of towers and water damns'', *12th FIG Symposium*. Baden, 2006, viewd 8 November 2014, [https://www.fig.net/resources/proceedings/2006/baden\\_2006\\_comm6/PDF/LS2/Schneider.pdf](https://www.fig.net/resources/proceedings/2006/baden_2006_comm6/PDF/LS2/Schneider.pdf)
- Teza, G., Galgaro, A, Zaltron, N & Genevois, R 2007, 'Terrestrial laser scanner to detect landslide displacement fields: a new approach', *International Journal of Remote Sensing*, pp. 3425–3446.
- Teza, G, & Pesci, A 2013, 'Geometric characterization of a cylinder-shaped structure from laser scanner data: Development of an analysis tool and its use on a leaning bell tower', *Journal of Cultural Heritage*, pp. 411–423.
- Tsakiri, M, Lichti, D & Pfeifer, N 2006, 'Terrestrial laser scanning for deformation monitoring', *12th FIG Symposium*. Baden, 2006, viewed 13 November 2014, [https://www.fig.net/resources/proceedings/2006/baden\\_2006\\_comm6/PDF/LS2/Tsakiri.pdf](https://www.fig.net/resources/proceedings/2006/baden_2006_comm6/PDF/LS2/Tsakiri.pdf)
- Vežočník, R, Ambrožič, T, Sterle, O, Bilban, G, Pfeifer, N, & Stopar, B 2009, 'Use of terrestrial laser scanning technology for long term high precision deformation monitoring', *Sensors*, pp. 9873-9895.
- Wei, Z, Huadong, G, Qi, L & Tianhua, H 2014, 'Fine deformation monitoring of ancient building based on terrestrial laser scanning technologies', *International Symposium on Remote Sensing of Environmen*, 2014, viewed 26 November 2014, <http://iopscience.iop.org/article/10.1088/1755-1315/17/1/012166/pdf>
- Wilkinson, M.W, McCaffrey, K.J.W, Roberts, G.P., Cowie, P.A., Phillips, R.J., Degasperri, M, Vittori, A, M, & Michetti, A, M 2012, 'Distribution and magnitude of post-seismic deformation of the 2009 L'Aquila earthquake (M6.3) surface rupture measured using repeat terrestrial laser scanning', *Geophysical Journal International*, pp. 911–922.